The Journal of Neuroscience, November 1, 2001, *21*(21):8482–8494

The Nonuniform Distribution of the $GABA_A$ Receptor α1 Subunit Influences Inhibitory Synaptic Transmission to Motoneurons within a Motor Nucleus

Jennifer A. O'Brien and Albert J. Berger

Department of Physiology and Biophysics, University of Washington, Seattle, Washington 98195-7290

Using immunohistochemistry we studied the distribution of $GABA_A$ and glycine receptor α1 subunits in the rat hypoglossal nucleus during postnatal development. In the neonate [postnatal day (P) 1–3] and adult nucleus (P28–30), $GABA_A$ receptor α1 subunit labeling was relatively modest. However, in the juvenile nucleus (P9–13), labeling was strong in the ventrolateral region and moderate in the dorsal region. Glycine receptor α1 subunit labeling was strong and uniform in the juvenile and adult nucleus and absent in the neonate nucleus. GABA and glycine neurotransmitter labeling was uniform throughout the neonatal and juvenile nucleus. To study the functional consequences of this regional differential $GABA_A$ receptor α1 subunit distribution, we voltage clamped juvenile hypoglossal motoneurons (HMs) from the ventrolateral and dorsal regions and recorded spontaneous miniature IPSCs (mIPSCs). Pure GABAergic events had slower decay times than glycinergic events. Although pure GABAergic and glycinergic decay times did not differ depending on HM location, the decays of mixed mIPSCs from ventrolateral HMs, recorded without $GABA_A$ and glycine receptor antagonists, had significantly slower decays than mIPSCs from dorsal HMs. Focally applied GABA and glycine onto outside-out patches revealed that the GABAergic to glycinergic peak current amplitude ratio was larger for patches from ventrolateral HMs compared with dorsal HMs. Dual component mIPSCs, presumably caused by co-release of GABA and glycine, were recorded more frequently in the ventrolateral nucleus. These data suggest that the number of synapses using $GABA_A$ receptor-mediated transmission is greater on ventrolateral HMs than dorsal HMs, demonstrating a nonuniformity of synaptic function within a defined motor nucleus.

Key words: glycine receptor; glycine; GABA; synaptic transmission; immunohistochemistry; $GABA_A$ receptor; inhibition; hypoglossal motoneurons; hypoglossal nucleus; dorsal motor nucleus of vagus; brainstem

GABA and glycine are the two main inhibitory neurotransmitters in the CNS, each activating a different family of ligand-gated ion channels. Although GABA is the main inhibitory neurotransmitter in the brain, both GABA and glycine can contribute to inhibition of single neurons in the brainstem and spinal cord (Jonas et al., 1998; O'Brien and Berger, 1999). In the developing spinal cord and brainstem, the overall contribution of each neurotransmitter to total inhibition of neurons can change (Gao and Ziskind-Conhaim, 1995; Kotak et al., 1998). Specifically during development, the amounts of GABA or glycine expressed (Simon and Horcholle-Bossavit, 1999) and changes in the inhibitory postsynaptic receptor density, distribution, and subunit composition can occur (Fritschy et al., 1994; Kotak et al., 1998; Singer et al., 1998).

Hypoglossal motoneurons (HMs) are located in the brainstem and innervate the tongue, which is involved in several motor functions, including mastication, swallowing, sucking, and speech (Lowe, 1980). It is also important for respiration, because it has a critical position in the upper airway. HMs are inhibited by both GABA and glycine *in vivo* (Altmann et al., 1972; Takata and Ogata, 1980). Experiments have shown that activation of orofacial afferents evoke glycinergic and GABAergic currents in HMs, suggesting that these currents have important functions associated with activation of orofacial sensory inputs (Sumi, 1969; Sumino and Nakamura, 1974). Several airway-related diseases may involve alterations in function of these motoneurons, including sleep apnea and sudden infant death syndrome (Konrat et al., 1992). Studies in humans have suggested that increased glycinergic inhibitory synaptic transmission to HMs may be a contributing factor in obstructive sleep apnea during REM sleep (Remmers et al., 1980; Yamuy et al., 1999). Thus understanding inhibition to HMs may lead to a better understanding of airway-related diseases.

At the cellular level, in neonatal rats GABA and glycine are co-released onto HMs from the same presynaptic terminal (O'Brien and Berger, 1999). Studies of glycine receptor-mediated synaptic transmission during the first few weeks of development have demonstrated a subunit switch of this receptor leading to a decrease in the miniature IPSC (mIPSC) decay times (Singer et al., 1998). Also, during development there is an increase in the number of glycine receptors at each synapse, leading to an increase in the mIPSC response amplitude (Singer and Berger, 1999). Changes in the expression of the $GABA_A$ and glycine receptors may influence the effect of these inhibitory neurotransmitters and thereby influence motor output throughout the first weeks of postnatal development. Therefore, we used immunohistochemistry and electrophysiology to study in HMs the relative

Received June 7, 2001; revised Aug. 17, 2001; accepted Aug. 22, 2001.

J.A.O. was supported by National Institutes of Health (NIH) Training Grant 5T32GM07108. This research was supported by NIH Grants HL-49657 and NS-14857 to A.J.B. We thank Dr. David Pow (University of Queensland, Australia) for the gift of the GABA and glycine neurotransmitter antibodies courtesy of Dr. Anita Hendrickson (University of Washington). We also thank Paulette Brunner for her assistance with the confocal microscopy. We are grateful to Mark Mazurek, Erika Eggers, and Rebecca Lim for reading and commenting on this manuscript and Dr. William Satterthwaite and Phan Huynh for technical assistance.

Correspondence should be addressed to Dr. Albert J. Berger, Department of Physiology and Biophysics, University of Washington, Box 357290, Seattle, WA 98195-7290. E-mail: berger@u.washington.edu

Copyright © 2001 Society for Neuroscience 0270-6474/01/218482-13$15.00/0

contributions of GABAergic and glycinergic inhibitory synaptic transmission, and we primarily focused on the intermediate stage of postnatal development [postnatal day (P) 9–13]. Our results suggest that at this age the relative contribution of $GABA_A$ receptor-mediated synaptic transmission varied throughout the hypoglossal nucleus.

MATERIALS AND METHODS

Primary antibodies. To study the distribution of the $GABA_A$ receptors in the hypoglossal nucleus, we used an antibody directed against the first 15 amino acids of the rat $GABA_A$ receptor α1 subunit (Upstate Biotechnology, Lake Placid, NY) (Vitorica et al., 1990). Two different aliquots of this antibody were used at the following dilutions: 1:750 and 1:75. To study the glycine receptor distribution, we used a monoclonal (mouse) antibody directed against the first 10 amino acids of the rat glycine receptor α1 subunit (Alexis Corporation, San Diego, CA) at a dilution of 1:100 (Pfeiffer et al., 1984). To study the distribution of choline acetyltransferase (ChAT) in the hypoglossal nucleus, we used a monoclonal antibody at a dilution of 1:100 (Chemicon, Temecula, CA) (Crawford et al., 1982). The distribution of GABA and glycine neurotransmitter was studied using polyclonal antibodies to GABA and glycine at dilutions of 1:750 and 1:2000, respectively (gift from D. Pow; University of Queensland, Australia) (Pow et al., 1995).

Immunohistochemistry. For all immunohistochemical experiments, Sprague Dawley rats were anesthetized by injection (intramuscular) of a ketamine–xylazine mixture (200 and 14 mg/kg, respectively). Rats were separated into three age groups: P1–3 (neonatal), P9–13 (juvenile), and P28–30 (adult). After decapitation, the brainstems were removed.

For double-label studies of the $GABA_A$ receptor α1 subunit and the glycine receptor α1 subunit, brainstems were frozen on dry ice. Transverse brainstem sections were cut using a cryostat (20–30 μm thick). Tissues were then fixed in 4% paraformaldehyde (Ted Pella, Redding, CA) in PBS for 10–20 min. The slide-mounted tissue sections were then incubated in PBS blocking solution containing 0.2% Triton X-100 (Sigma, St. Louis, MO) and 10% donkey serum (Vector Laboratories, Burlingame, CA) for 1 hr at room temperature. Slices were placed overnight in a PBS blocking solution containing the primary antibodies at 4°C. After washing in PBS, tissue sections were incubated in secondary antibodies Cy3-conjugated anti-rabbit IgG (1:600; Jackson ImmunoResearch Laboratories, West Grove, PA) and biotin-SP-conjugated anti-mouse IgG (1:200; Jackson ImmunoResearch Laboratories) in PBS blocking solution for 90 min at room temperature. After washing, tissue sections were incubated in Fluorescein Avidin D (1:500; Vector Laboratories) for 60 min at room temperature. The slides were then coverslipped with Vectashield (Vector Laboratories).

For single-label studies of GABA and glycine neurotransmitter, as well as double-label studies of $GABA_A$ receptor α1 subunit and ChAT, transverse brainstem slices were cut using a vibratome (300–700 μm thick). During slicing, the brainstems were immersed in an ice-cold Ringer's solution containing (in mM): 119 NaCl, 26.2 $NaHCO_3$, 1 NaH_2PO_4, 2.5 KCl, 11 glucose, 2.5 $CaCl_2$, and 1.4 $MgSO_4$ bubbled with 95% O_2/5% CO_2 gas mixture. These sections were fixed in 4% paraformaldehyde in PBS for 1–3 d. After fixation, slices were cryoprotected by suspending them overnight in a PBS solution containing 30% sucrose at 4°C overnight. The slices were then resectioned on a freezing microtome (40–50 μm thick).

Free-floating tissue sections were made permeable and blocked in PBS blocking solution for 1 hr at room temperature. Overnight incubation with the primary antibodies was performed in PBS blocking solution at 4°C. For single-label studies of GABA and glycine, tissues were incubated with the secondary antibody (1:600 Cy3-conjugated anti-rabbit IgG; Jackson ImmunoResearch Laboratories) in PBS blocking solution for 90 min at room temperature. For the double-label studies of the $GABA_A$ receptor α1 subunit and ChAT, after incubation in the primary antibodies the tissue sections were incubated with Alexa Fluor 488 goat anti-rabbit IgG (1:200; Molecular Probes, Eugene, OR) and Alexa Fluor 568 anti-mouse IgG (1:200; Molecular Probes) in PBS blocking solution for 1 hr at room temperature. Sections were then placed on slides and coverslipped with Vectashield.

Immunohistochemistry on recorded neurons. In a number of electrophysiological experiments, a single neuron in each slice was filled with 0.1–0.5% Lucifer yellow (Sigma) or Alexa Fluor 488 (100–250 μM; Molecular Probes). After recordings, slices were fixed overnight in 4% paraformaldehyde in PBS. Slices (300 μm thick) were placed in 30% sucrose and then resectioned using a freezing microtome (75 μm thick). The free-floating slice containing the filled neuron was incubated in 0.2% Triton X-100 and 10% donkey serum for 1 hr at room temperature, followed by overnight incubation with $GABA_A$ receptor α1 subunit antibody at 4°C. After washing, slices were incubated in the secondary antibody Cy3-conjugated anti-rabbit IgG (1:600) in PBS blocking solution for 90 min at room temperature. After washing, slides were coverslipped with Vectashield.

Confocal microscopy. Confocal sections were collected using either a Bio-Rad MRC-600 (Bio-Rad, Hercules, CA) or a Leica Spectral (Leica, Wetzlar, Germany) confocal microscope. For labeling with Cy3 or Alexa Fluor 568, images were obtained using 548 nm excitation wavelength. For Fluorescein and Alexa Fluor 488 labeling, images were obtained with 488 excitation wavelength. Images were Kalman filtered. Using PhotoShop 5.5 (Adobe, San Jose, CA), images were cropped, sized, and merged. Final figures were created in PowerPoint (Microsoft, Seattle, WA).

Electrophysiology. Sprague Dawley rats, separated into two age groups [neonatal (P1–3) and juvenile (P9–13)], were anesthetized by injection (intramuscular) of a ketamine–xylazine mixture (200 and 14 mg/kg, respectively). Rats were decapitated, brainstems were removed, and transverse brainstem slices (250–300 μm) were prepared using a vibratome. During slicing, incubation (1 hr at 37°C), and recording, the slices were bathed in a Ringer's solution containing (in mM): 119 NaCl, 26.2 $NaHCO_3$, 1 NaH_2PO_4, 2.5 KCl, 11 glucose, 2.5 $CaCl_2$, and 1.4 $MgSO_4$. Solutions were bubbled continuously with 95% O_2/5% CO_2 gas mixture. Using near-infrared DIC optics, HMs were identified on the basis of their characteristic location and morphology (Umemiya and Berger, 1994).

Whole-cell patch-clamp and outside-out patch recordings were performed at room temperature. Patch electrodes (resistance 1–5 MΩ) were filled with (in mM): 145 CsCl, 10 HEPES, 10 EGTA, 2 $MgCl_2$, 2 ATP-Mg, 0.2 GTP-Tris, pH 7.2. For mIPSC experiments, HMs were voltage clamped at −55 to −65 mV. Access resistance was uncompensated and always <20 MΩ and was monitored throughout the experiment. Data were filtered at 2 kHz and digitized at 5 kHz using pCLAMP software (Axon Instruments, Foster City, CA). To test for the selectivity of bicuculline and strychnine, glycine (200 μM) and GABA (200 μM) were applied (10–50 msec) using a dual-channel Picospritzer (General Valve, Fairfield, NJ) and a single-barrel glass pipette (World Precision Instruments, Sarasota, FL). For measurements of the responses, five current traces were averaged, and peak current amplitude was measured using pCLAMP 6.0, 7.0, or 8.0 software (Axon Instruments). These experiments were performed in the presence of tetrodotoxin (TTX; 0.5–1 μM) and 6,7-dinitroquinoxaline (DNQX; 10–20 μM) to block Na^+-dependent action potentials and non-NMDA glutamate receptors, respectively.

For outside-out patch recordings, a double-barrel pipette was used to focally apply for 3 sec glycine (200 μM) or GABA (200 μM) onto excised patches. Patches were voltage clamped at −30 mV during application of glycine and GABA. These experiments were performed in the presence of TTX (0.5–1 μM) and DNQX (10–20 μM). For comparison of data within an experiment, all patches were excised from the same slice so that glycine and GABA could be applied using only one double-barrel puffer pipette. The puffer pipette was visualized and kept secure in one location so that multiple patches from a single slice could be aligned with the puffer pipette in the same way for application of glycine and GABA.

Glycinergic mIPSCs were recorded in the presence of TTX (1 μM), DNQX (20 μM), D(−)-2-amino-5 phosphopentanoic acid (AP5; 25–50 μM), and bicuculline (5 μM). GABAergic mIPSCs were recorded in the presence of the same blockers, except that bicuculline was replaced with strychnine (1 μM). We measured the mIPSC peak amplitude, the time it took for mIPSC to decay to 37% of its peak amplitude, and the 10–90% rise time of the mIPSC. Spontaneous mIPSCs were analyzed by software developed in our laboratory that detects events using an algorithm described by Cochran (1993). A minimum of 100 events were analyzed for each neuron. Decay times were measured as the time for the mIPSC to decay to 37% of its peak amplitude. Results are presented as mean ± SEM unless noted otherwise. The Kolmogorov–Smirnov statistical test was used to assess differences in mIPSC data. An unpaired *t* test was used to assess differences in mean values from different conditions. Changes were considered significant if $p < 0.05$. Data plotted as histograms were fitted with Gaussian curves using SigmaPlot (SPSS, Chicago, IL).

The drugs that were used included bicuculline methiodide (Sigma), strychnine hydrochloride (Sigma), TTX (Alomone Labs, Jerusalem, Is-

rael), DNQX (RBI, Natick, MA), AP5 (RBI), and sodium pentobarbital (Abbott Labs, North Chicago, IL).

RESULTS

Distribution of $GABA_A$ α1 and glycine α1 receptor subunits in the developing hypoglossal nucleus

To better understand the developmental progression of $GABA_A$ receptors in the hypoglossal nucleus, we studied changes in the α1 $GABA_A$ receptor subunit throughout postnatal development. We used an antibody that recognized the α1 subunit of the $GABA_A$ receptor, because immunohistochemical studies have shown that in adult HMs α1, α2, and γ2 are the main subunits expressed, whereas β2/3, α3, α5, and α6 expression was reported to be absent (Fritschy and Mohler, 1995). A recent immunohistochemical study of the neonatal hypoglossal nucleus (P1–5) found that α2 subunit staining was present, whereas α1 staining was reported to be absent (Donato and Nistri, 2000).

We found that $GABA_A$ receptor α1 subunit staining in the neonatal (P1–3) hypoglossal nucleus was weak throughout the caudal and rostral extent of the nucleus (Fig. 1*A*, *XII*). The dorsal motor nucleus of vagus stained moderately for the $GABA_A$ receptor α1 subunit (Fig. 1*A*, *X*). In the juvenile (P9–13) hypoglossal nucleus, the degree of $GABA_A$ receptor α1 subunit staining depended on location throughout the nucleus (Fig. 1*B*, *XII*). Specifically throughout the caudal to middle regions of the hypoglossal nucleus, the $GABA_A$ receptor α1 subunit staining was strongest in the ventrolateral region (Fig. 1*B*, *arrow*). In contrast, throughout the entire caudal to rostral extent of the nucleus, weak to moderate staining was seen in the dorsal and ventromedial regions. Additionally, at this postnatal age the dorsal motor nucleus of the vagus had strong staining (Fig. 1*B*, *X*). In the adult hypoglossal nucleus (P25–30), the $GABA_A$ receptor staining was weak throughout its entire caudal and rostral extent, and strong staining was seen in the dorsal motor nucleus of the vagus (Fig. 1*C*).

To study glycine receptor expression, we used an antibody that detected the α1 subunit of the glycine receptor. Previous *in situ* hybridization experiments from our laboratory demonstrated that the glycine receptor α1 subunit is expressed in juvenile but absent in neonate HMs, whereas the α2 subunit is expressed in neonate but absent in juvenile HMs. In contrast, the β subunit is expressed uniformly throughout postnatal development (Singer et al., 1998). To better understand the development of the glycine receptor α1 subunit, we studied its expression throughout the postnatal period.

In neonatal animals (P1–3), very little glycine receptor α1 subunit staining was seen in the hypoglossal or dorsal motor nucleus of the vagus (Fig. 2*A*) ($n = 4$). However, in the juvenile (P9–13) and adult (P28–30) age groups, antibodies to the α1 subunit labeled the hypoglossal nucleus uniformly, whereas staining was virtually absent in the dorsal motor nucleus of the vagus (Fig. 2*B*,*C*) ($n \geq 4$ for each group). These data show that compared with the neonate hypoglossal nucleus, the glycine receptor α1 subunit is uniformly present at increased levels throughout the juvenile and adult nucleus, thus agreeing with the previous study from our laboratory using *in situ* hybridization (Singer et al., 1998).

Next we studied colocalization of the $GABA_A$ and glycine receptor α1 subunits in the juvenile hypoglossal nucleus by performing double labeling. $GABA_A$ receptor α1 subunit labeling (Fig. 3*A*, *red*) and glycine receptor α1 subunit labeling (Fig. 3*B*, *green*) from the same tissue section are shown as a merged image in Figure 3*C*. At higher magnification of the ventrolateral region,

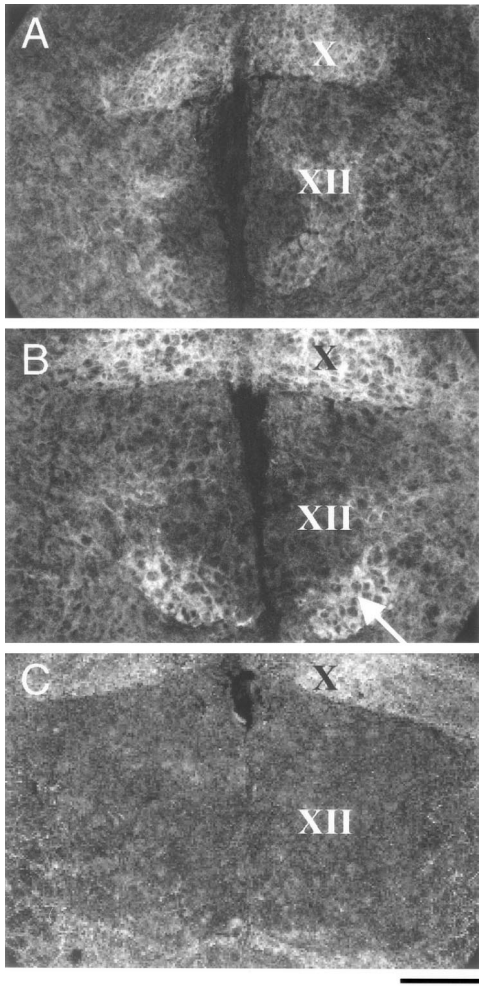

Figure 1. Labeling of the hypoglossal nucleus for the $GABA_A$ receptor α1 subunit in neonate (P2), juvenile (P11), and adult (P30) rat. *A*, In the neonate, $GABA_A$ receptor α1 subunit labeling was weak throughout the hypoglossal nucleus (*XII*) and moderate in the dorsal motor nucleus of the vagus (*X*) ($n = 4$). *B*, In the juvenile, $GABA_A$ receptor α1 subunit labeling was strongest in the ventrolateral region of the hypoglossal nucleus (*arrow*) and dorsal motor nucleus of the vagus, moderate in the dorsal region of the hypoglossal, and weakest in the ventromedial region of the hypoglossal nucleus ($n = 5$). *C*, In the adult, $GABA_A$ receptor α1 subunit staining is modest in the hypoglossal nucleus and strong in the dorsal motor nucleus of the vagus ($n = 5$). Scale bar, 200 μm.

colocalization of the $GABA_A$ and glycine receptor α1 subunits is present (Fig. 3*D*, *orange*). In the dorsal and ventromedial areas of the nucleus, double labeling of the two receptors types was not obvious because of the weaker staining of $GABA_A$ receptor α1 subunit as opposed to the stronger glycine receptor α1 subunit staining. Double labeling of the neonate and adult hypoglossal nucleus was also performed; however, because of weak labeling of the $GABA_A$ receptor α1 subunit at these ages, colocalization of the two receptor types was not apparent (data not shown) ($n \geq 4$ for all groups).

To confirm that the differential $GABA_A$ receptor α1 subunit staining was present within the hypoglossal nucleus on juvenile HMs, we labeled HMs with choline acetyltransferase (Fig. 4*A1*, *ChAT*) to identify motoneurons. Double labeling of $GABA_A$ receptor α1 subunit and ChAT showed that $GABA_A$ receptor α1 subunit labeling was present on HMs in the ventrolateral region of the hypoglossal nucleus (Fig. 4*A3*,*B1*). At this high power of

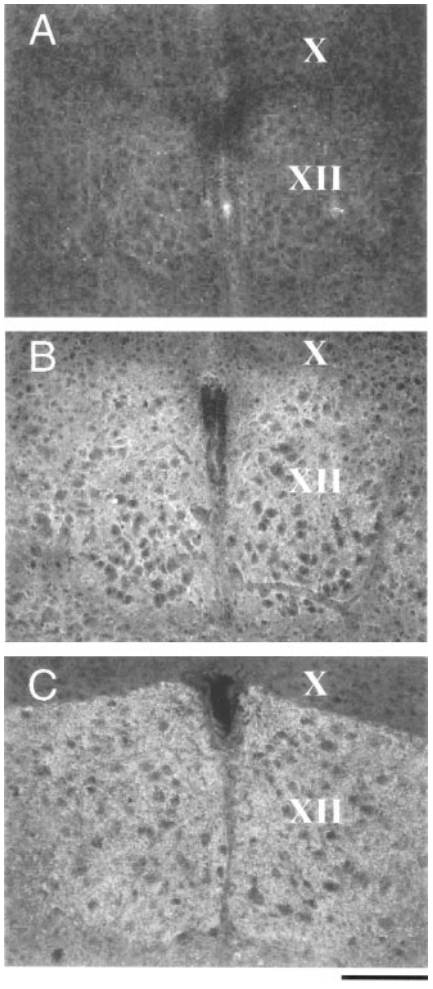

Figure 2. Labeling of the hypoglossal nucleus for the glycine receptor α1 subunit in neonate (P2), juvenile (P11), and adult (P30) rat. *A*, In the glycine receptor α1 subunit, labeling is faint and diffuse throughout the hypoglossal nucleus (*XII*) and dorsal motor nucleus of vagus (*X*). *B*, *C*, In both the juvenile and adult, glycine receptor α1 subunit labeling is strong throughout the entire hypoglossal nucleus (*XII*) and virtually absent from the dorsal motor nucleus of the vagus (*X*). Scale bar, 200 μm.

resolution, each of the neuronal somata labeled with ChAT was surrounded with $GABA_A$ receptor α1 subunit labeling. These data indicated that some of the $GABA_A$ receptor staining in this region was probably directly on HMs. In contrast, $GABA_A$ receptor α1 subunit labeling in the ventromedial and dorsal regions of the hypoglossal nucleus was less intense (Fig. 4*B2*,*B3*). HMs in these regions were not surrounded by the dense staining observed in the ventrolateral region. These differences in $GABA_A$ receptor α1 subunit labeling were found in all five hypoglossal nuclei double labeled with ChAT and $GABA_A$ receptor α1 subunit antibodies.

Distribution of GABA and glycine neurotransmitters in the hypoglossal motor nucleus

We studied the distribution of glycine and GABA neurotransmitter using antibodies that recognized the neurotransmitters. In the neonate (P1–3) and juvenile (P9–13), GABA staining was present uniformly throughout the hypoglossal nucleus (Fig. 5*A1*,*A2*, *XII*). This pattern of staining was also present in adult HMs (P25–30; data not shown). Glycine staining was also present uniformly throughout the hypoglossal motor nucleus (Fig. 5*B1*,*B2*, *XII*).

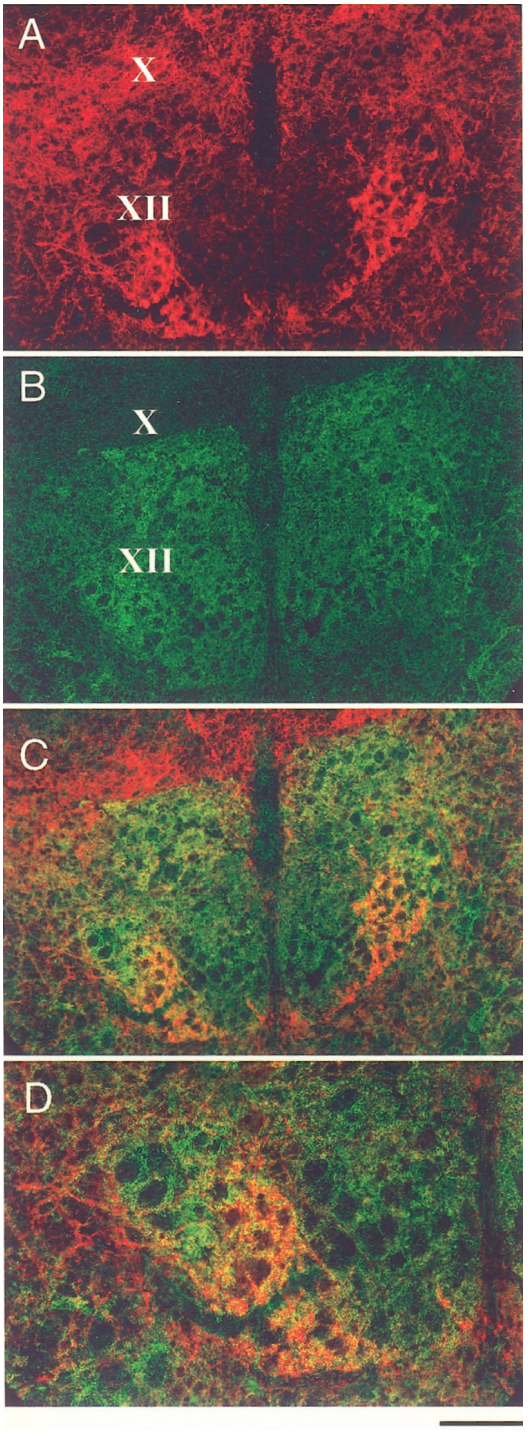

Figure 3. *A*, *B*, Staining for the $GABA_A$ receptor α1 subunit (*A*, *red*) and glycine receptor α1 subunit (*B*, *green*) in the same tissue section of the hypoglossal nucleus (*XII*) from a juvenile rat. *C*, Images from *A* and *B* are shown merged. $GABA_A$ receptor α1 subunit labeling differs depending on location within the hypoglossal nucleus, whereas glycine receptor labeling is uniform throughout the nucleus. There is dense $GABA_A$ receptor α1 subunit labeling of the ventrolateral region of the hypoglossal nucleus. *D*, At higher magnification, colocalization of $GABA_A$ and glycine receptor α1 subunits was seen (*orange*). Tissues shown are from the same animal (P10) and are representative of data obtained from five different animals. Scale bar: *A–C*, 200 μm; *D*, 100 μm.

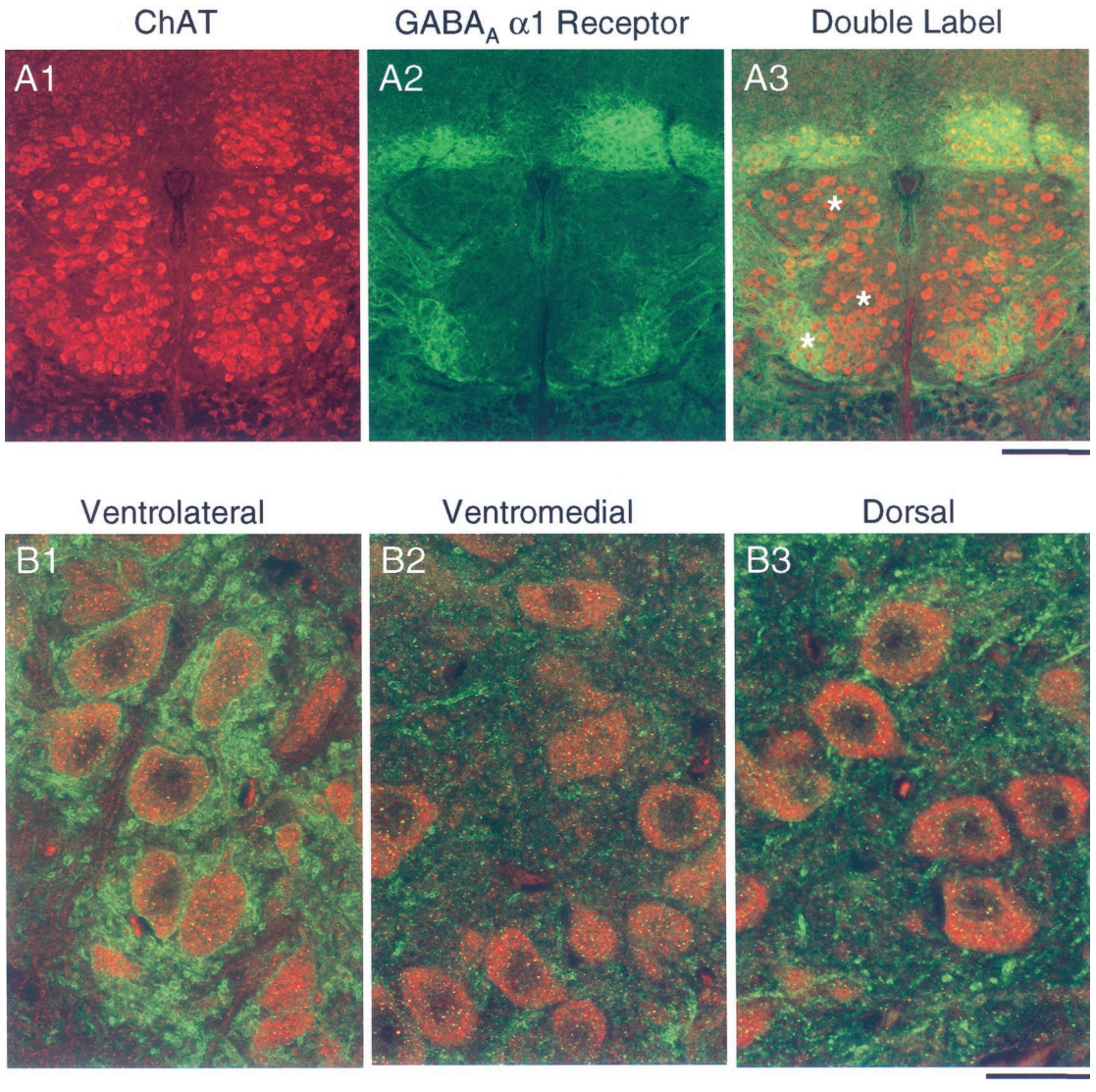

Figure 4. Double labeling of the hypoglossal nucleus for the $GABA_A$ receptor α1 subunit and ChAT in a juvenile (P10) rat. *A1*, ChAT labeling of neurons in the hypoglossal and dorsal motor nucleus of vagus. *A2*, $GABA_A$ receptor α1 subunit labeling is strongest in the ventrolateral region of the hypoglossal motor nucleus and dorsal motor nucleus of the vagus and weakest in the dorsal region of the hypoglossal and the ventromedial region of the hypoglossal nucleus ($n = 5$). *A3*, Double label of $GABA_A$ receptor α1 subunit (*green*) and ChAT (*red*) in the hypoglossal nucleus. Scale bar, 200 μm. *B1–B3*, Higher magnification of the hypoglossal nucleus from the regions denoted with *asterisks*. At higher magnification, $GABA_A$ receptor α1 subunit labeling on HMs was greatest in the ventrolateral region (*B1*), whereas in the ventromedial and dorsal regions, labeling was much less intense (*B2* and *B3*, respectively). Scale bar, 40 μm. These distributions were representative of all juvenile animals studied ($n = 5$).

These uniform distributions were seen throughout the caudal to rostral extent of the nucleus and were also present in adult HMs (P25–30; data not shown). Interestingly, the dorsal motor nucleus of the vagus exhibited staining for GABA in both age groups (Fig. 5*A1*,*A2*, *X*) but absent to weak glycine staining in both age groups (Fig. 5*B1*,*B2*, *X*).

Glycinergic and GABAergic responses of juvenile rats

We next studied the inhibitory properties of juvenile HMs recorded from different regions of the hypoglossal nucleus. We focused on this age because the staining for $GABA_A$ receptor α1 subunit varied within the nucleus at this age group in contrast to other ages studied. We were interested in comparing the relative contribution of GABA and/or glycine to inhibitory synaptic transmission throughout different regions of the juvenile nucleus.

We compared $GABA_A$ and glycine receptor-mediated synaptic responses by recording spontaneous mIPSCs in different regions of the nucleus. Recorded spontaneous mIPSCs are caused by release of single vesicles of neurotransmitter from presynaptic terminals (Katz, 1969; Isaacson and Walmsley, 1995). Properties of mIPSCs, including the amplitude, rise times, and decay times, often depend on the density and type of postsynaptic receptors present at the synapse. In a previous study of neonatal HMs, we recorded both $GABA_A$ receptor-mediated mIPSCs and glycine receptor-mediated mIPSCs (O'Brien and Berger, 1999). The GABAergic mIPSCs had significantly slower decay times than the glycinergic mIPSCs. The distinct kinetics of the $GABA_A$ and glycine receptor-mediated responses allowed us to record dual component mIPSCs that were mediated by both receptor subtypes in the neonate. If these findings were also present in

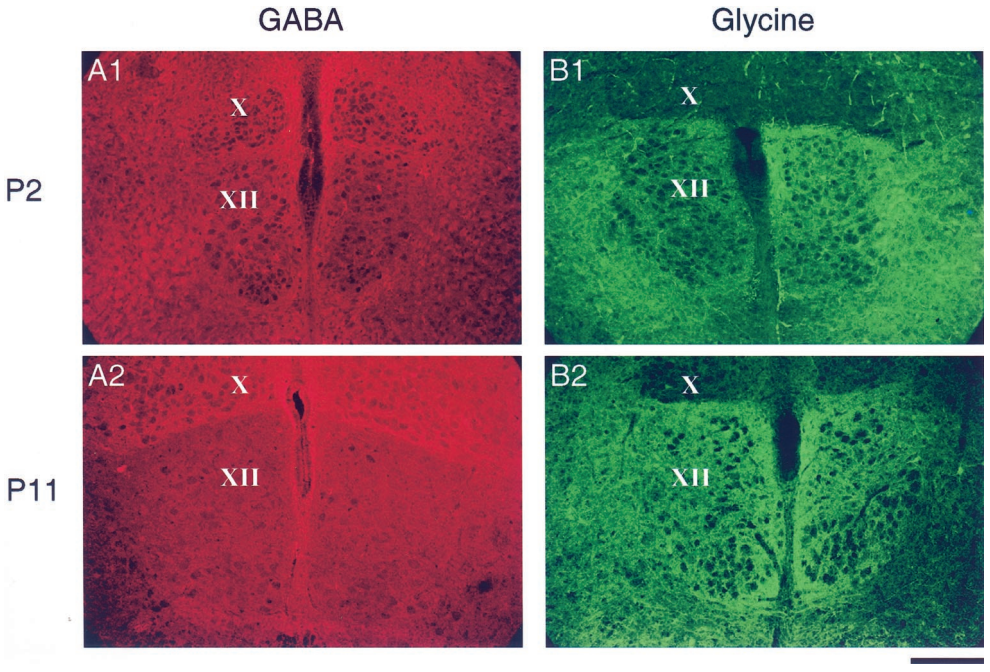

Figure 5. Antibody labeling for GABA and glycine in neonate (*P2*) and juvenile (*P11*) rat hypoglossal nuclei. *A1*, In the neonate GABA labeling was present to a similar degree in both the hypoglossal nucleus and the dorsal motor nucleus of the vagus ($n = 3$). *A2*, In the juvenile there was moderate uniform labeling of the hypoglossal nucleus and uniform but denser labeling of the dorsal motor nucleus of the vagus ($n = 5$). *B1*, *B2*, In the neonate (*B1*) and juvenile (*B2*), glycine labeling is dense and uniform throughout the hypoglossal nucleus ($n = 3$ for neonates and $n = 5$ for juvenile). In contrast, at both ages studied the dorsal motor nucleus of the vagus is labeled weakly by the glycine antibody. Scale bar, 200 μm.

Table 1. Comparison of mIPSC properties recorded in juvenile hypoglossal motoneurons

	Events recorded in the absence of pentobarbital				Events recorded in the presence of pentobarbital			
Types of mIPSCs	Decay (msec)	Amplitude (pA)	Rise time (msec)	*n*	Decay (msec)	Amplitude (pA)	Rise time (msec)	*n*
Control	13.0 ± 4.3	51.1 ± 25.0	1.5 ± 0.1	13	33.2 ± 14.4	51.5 ± 12.2	1.8 ± 0.3	16
GABA	19.5 ± 7.3*	41.3 ± 12.7	1.8 ± 0.4	13	66.3 ± 21.2*	38.8 ± 20.4	3.0 ± 0.6	9
Glycine	6.9 ± 3.3	52.9 ± 19.9	1.3 ± 0.4	13	9.3 ± 2.4	55.2 ± 20.9	1.5 ± 0.2	6

Values are means ± SD. Decay kinetics were measured as the time for mIPSC to decay to 37% of its peak amplitude.
*GABAergic mIPSC decay times were significantly prolonged by pentobarbital ($p \leq 0.05$; *t* test). *n* indicates the number of cells studied.

juvenile HMs, it would be possible to record and compare the $GABA_A$ and glycine receptor contribution to mIPSCs in single HMs. Specifically, mIPSCs mediated by synapses with a larger ratio of $GABA_A$ receptors to glycine receptors at each synapse would, on average, have relatively slower decay times than mIPSCs mediated by synapses with a smaller ratio of $GABA_A$ receptors to glycinergic receptors. However, for this prediction to be true, we must also demonstrate that the properties of isolated $GABA_A$ receptor-mediated mIPSCs as well as glycine receptor-mediated mIPSCs did not differ in the different regions of the hypoglossal nucleus.

Before recording isolated GABAergic and glycinergic mIPSCs, we established the concentration of $GABA_A$ receptor antagonist (bicuculline) and glycine receptor antagonist (strychnine) that selectively isolate $GABA_A$ or glycine receptor-mediated responses in juvenile HMs. To do this we focally applied GABA and glycine onto an HM, and then bicuculline or strychnine were bath applied. In all cells from juvenile rats, focal application of GABA or glycine produced a current ($V_h = -60$ mV; data not shown). Bath application of 5 μM bicuculline blocked 87 ± 11.6% (mean ± SD) of the $GABA_A$ receptor-mediated current ($n = 4$), whereas it blocked only 7 ± 5.0% of the glycine receptor-mediated current ($n = 3$). Bath application of 1 μM strychnine blocked 91 ± 5.0% of the glycine receptor-mediated current ($n = 3$), whereas it inhibited the $GABA_A$ receptor-mediated current by only 17 ± 9.7% ($n = 3$). These data show that 5 μM bicuculline can selectively block the majority of $GABA_A$ receptor-mediated responses, without having a large effect on the glycine receptor-mediated responses. These data also show that 1 μM strychnine can selectively block the majority of the glycine receptor-mediated response, without largely inhibiting $GABA_A$ receptor-mediated response.

We next studied the $GABA_A$ and glycine receptor-mediated synaptic responses in tissue from juvenile animals. Pure GABAergic and glycinergic mIPSCs were each recorded in isolation. We measured the mIPSC peak amplitude, the time it took for mIPSC to decay to 37% of its peak amplitude, and the 10–90% rise time of the mIPSC. These data are summarized in Table 1. On average, the $GABA_A$ receptor-mediated current decay times were significantly slower than the glycinergic mIPSCs. Average GABAergic and glycinergic decay times were 19.5 ± 7.3 msec ($n = 13$) and 6.9 ± 3.3 msec ($n = 13$), respectively (mean ± SD; $p < 0.005$).

To further enhance the differences in GABAergic and glycinergic decay times, we recorded mIPSCs in the presence of pentobarbital (25 μM). Previously we showed in neonatal HMs that $GABA_A$ receptor-mediated mIPSCs recorded in the presence of pentobarbital have significantly longer decay times than glycine receptor-mediated mIPSCs (O'Brien and Berger, 1999). In juvenile HMs we found that pentobarbital significantly slowed the decay kinetics of GABAergic mIPSCs in the juvenile HMs,

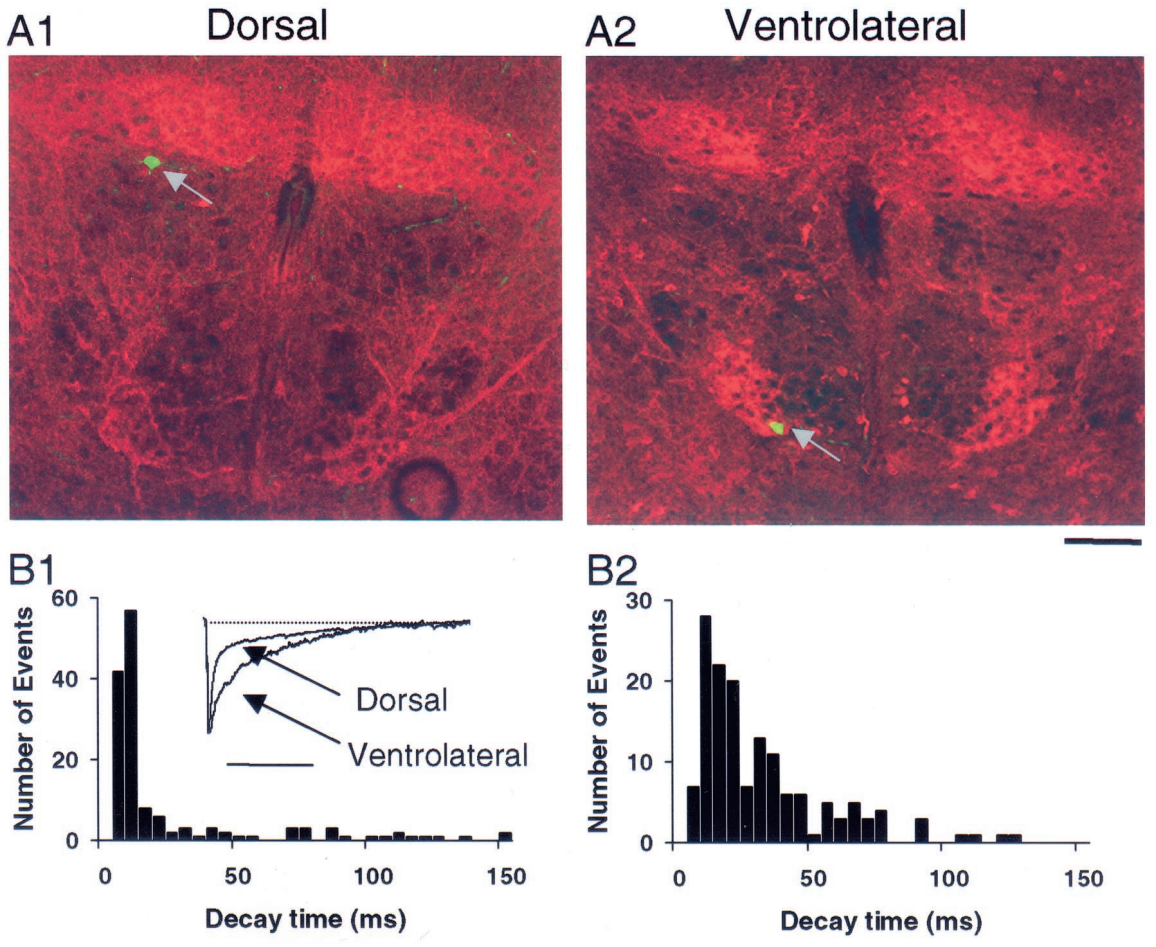

Figure 6. Mixed mIPSCs recorded from HMs located in the ventrolateral region have slower decay times than mIPSCs from HMs located in the dorsal region of the hypoglossal nucleus. *A1*, *A2*, Two slices are shown, each with a single HM labeled with Lucifer yellow during mIPSC recordings (*gray arrows*). After recordings, these sections were labeled with antibody that recognized $GABA_A$ receptor α1 subunit. The HM in A1 is located in the dorsal region of the hypoglossal nucleus, and the HM in A2 is located in the ventrolateral region of the nucleus. Scale bar, 200 μm. *B1*, *B2*, Histogram distributions of mixed mIPSC decay times for the HMs shown in *A1* and *A2*, respectively. The decay times of the mIPSCs of the ventrolateral HM (*B2*) were significantly slower than the decay times of mIPSCs of the dorsal HM (*B1*). *Inset*, Average mIPSC normalized to the peak amplitude from the ventrolateral HM and the dorsal HM. Calibration: 100 msec.

whereas it had no significant effect on the decay kinetics of glycine receptor-mediated events (Table 1).

Inhibitory currents properties depend on location of hypoglossal motoneurons

Next, we recorded mIPSCs from HMs in identified regions of the hypoglossal nucleus of juvenile rats. During recordings, HMs were filled with a fluorescent dye to confirm the regions within the hypoglossal nucleus from which the recordings were made. After fixation, tissue was stained with the $GABA_A$ receptor α1 subunit antibody (Fig. 6*A1*,*A2*). These recordings were performed in the presence of pentobarbital (25 μM), TTX, and glutamate receptor blockers but in the absence of strychnine and bicuculline. Therefore, mIPSCs recorded under these conditions were caused by release of GABA and/or glycine at different synapses on the recorded HM.

Figure 6*B* shows the histogram distributions of the decay kinetics of the two HMs pictured in Figure 6*A*. The mIPSC decay kinetics of the HM from the ventrolateral region, where $GABA_A$ receptor staining is greatest (Fig. 6*A2*), was slower than the decay kinetics of the HM from the dorsal region, where $GABA_A$ receptor α1 subunit staining was less (Fig. 6*A1*). The mIPSC decay time distributions from the dorsal region was significantly different from the distribution from the ventrolateral region (Kolmogorov–Smirnov test; $p < 0.05$). The average decay time for the HM from the dorsal region was 21.5 ± 29.7 msec (mean ± SD) (Fig. 6*B1*). In contrast, the average decay time for the cell shown in the ventrolateral region was 28.7 ± 24.6 msec (Fig. 6*B2*). Also shown in Figure 6*B1* (*inset*) are averages of mIPSCs from each of the recorded HMs shown. The averaged mIPSCs were normalized to the peak response to better illustrate the differences in decay kinetics for these two HMs.

We consistently found that the average decay kinetics of mIPSCs, in the absence or presence of pentobarbital, was slower in HMs recorded from the ventrolateral region as compared with HMs from the dorsal region (Fig. 7*A*). Plotted in Figure 7*A* (*right panel*) is the average cumulative probability distribution of decay kinetics for mIPSCs recorded from dorsal and ventrolateral HMs, in the presence of pentobarbital. For each neuron studied, we also averaged the decay times of the individual events studied. These averaged values were then combined to obtain an average of all neurons studied (Fig. 7*A*, *left panel*). In the presence of pentobarbital, the mean decay times were 30.7 ± 1.5 msec

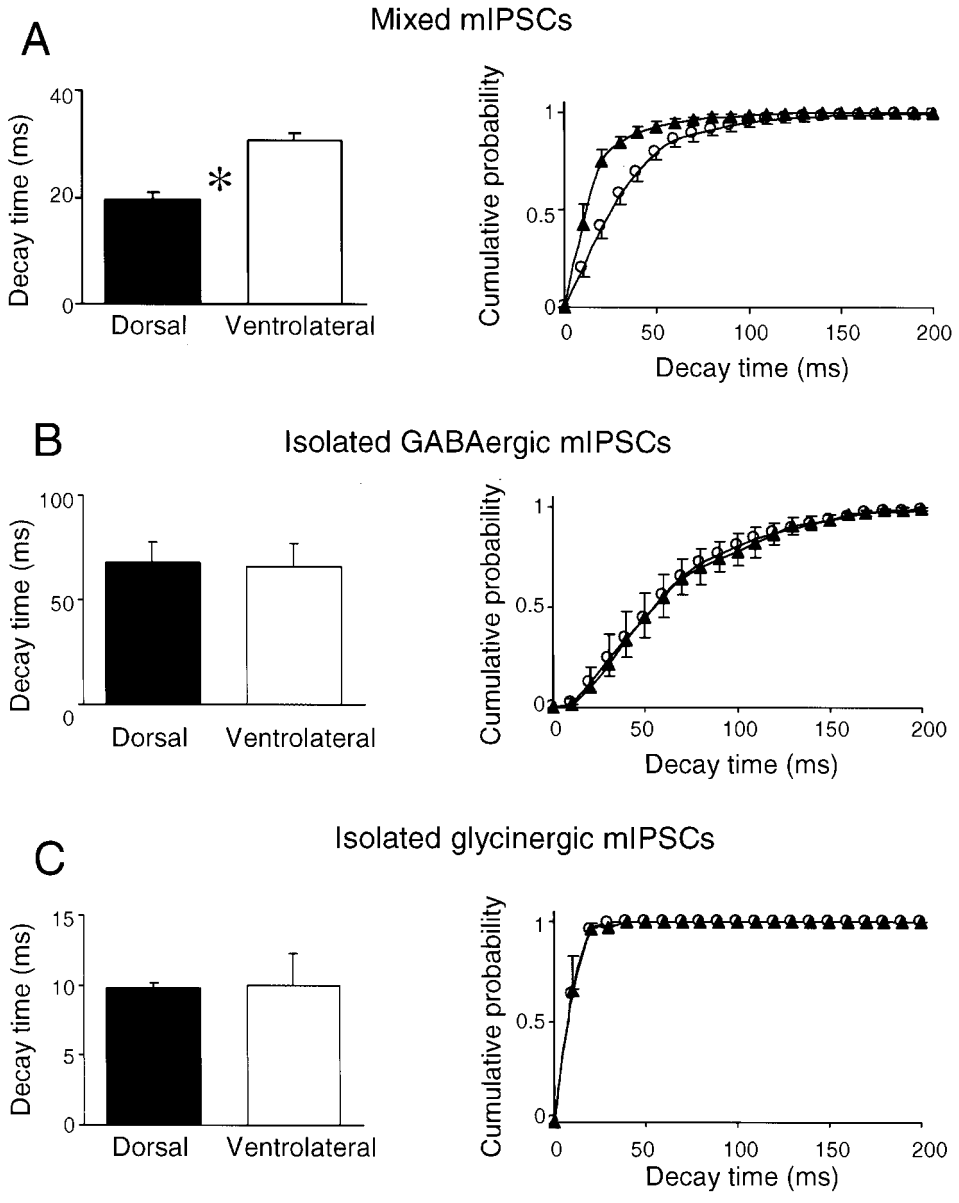

Figure 7. GABAergic/glycinergic mixed mIPSC decay times are slower in HMs from the ventrolateral region of the hypoglossal nucleus as compared with the dorsal region. In contrast, isolated GABAergic mIPSC decay times are similar in HMs from ventrolateral and dorsal regions. Also, isolated glycinergic mIPSCs decay times were similar in different HMs from the two regions of the nucleus. *A*, *Left*, Bar chart of the average mixed mIPSC decay times (±SEM) versus region. The average decay time was greater in the ventrolateral region. Regional differences in decay times were significant (*t* test; $^*p < 0.05$). *Right*, Averaged cumulative probability (±SEM) of GABAergic and glycinergic mIPSC decay times recorded in HMs from either the dorsal (▲) or ventrolateral (○) hypoglossal nucleus with pentobarbital (25 μM) present in the extracellular solution. Decay times of HMs in the ventrolateral region are shifted to the *right*, compared with those recorded in the dorsal region, indicating that a greater percentage of mIPSCs have slower decay kinetics. *B*, Pure GABAergic mIPSCs recorded in isolation (in the presence of strychnine). *Left*, The average pure GABAergic mIPSC decay times were not significantly different from HMs recorded in both regions ($n > 4$ for each group; *t* test; $p > 0.05$). *Right*, Cumulative probability of GABAergic decay times from the dorsal (▲) or ventrolateral (○) regions overlapped. Average values ± SEM are shown. *C*, *Left*, Pure glycinergic mIPSCs recorded in isolation (in the presence of bicuculline) on average were not significantly different. *Right*, Averaged cumulative probability of glycinergic mIPSC decay times from the dorsal (▲) or ventral regions (○) overlapped.

(mean ± SEM; $n = 8$) and 19.4 ± 1.3 msec ($n = 4$) in HMs from the ventrolateral and dorsal region, respectively. These means were significantly different ($p < 0.005$; *t* test). Additionally, we found for mixed mIPSCs recorded without pentobarbital that the decay kinetics were 16.0 ± 1.6 msec ($n = 7$) and 11.0 ± 1.2 msec ($n = 6$) in ventrolateral and dorsal HMs, respectively (mean ± SEM). These values were significantly different ($p < 0.05$).

GABAergic and glycinergic responses recorded in isolation

Although we predicted that differences in decay times were caused by differences in the ratio of GABAergic to glycinergic receptors at a synapse, we needed to confirm that pure $GABA_A$ receptor-mediated events as well as pure glycine receptor-mediated events were the same in each region. In both cases we found on average that the isolated GABAergic and the isolated glycinergic response characteristics did not differ when recorded from HMs in the two regions studied (Fig. 7*B*,*C*). For GABAergic mIPSCs recorded in the presence of pentobarbital, the average decay time was 66.1 ± 11.1 msec in the ventrolateral region and 67.9 ± 9.9 msec in the dorsal region (Fig. 7*B*, *left panel*) (mean ± SEM, $p > 0.1$). Shown in Figure 7*B* (*right panel*) is the averaged cumulative probability histogram of decay times recorded from HMs in the two regions. The average decay time of GABA mIPSCs recorded in the absence of pentobarbital was 19.0 ± 3.8 msec in the ventrolateral region and 20.2 ± 1.1 msec in the dorsal region ($n = 6$), and these also did not differ significantly (mean ± SEM; $p > 0.1$). Additionally, the amplitude and rise time of the pure GABAergic mIPSCs recorded in both conditions (with and without pentobarbital) did not differ depending on region (data not shown).

Similarly, the decay times of isolated glycinergic mIPSCs did not significantly differ depending on region. In the presence of pentobarbital, the average decay time was 10.0 ± 0.2 msec ($n = 3$) in the ventrolateral region and 9.8 ± 0.4 msec ($n = 3$) in the dorsal region (Fig. 7*C*, *left panel*) (mean ± SEM; $p > 0.1$). Shown in Figure 7*C* (*right panel*) is the averaged cumulative probability histogram of decay times recorded from HMs in the two regions.

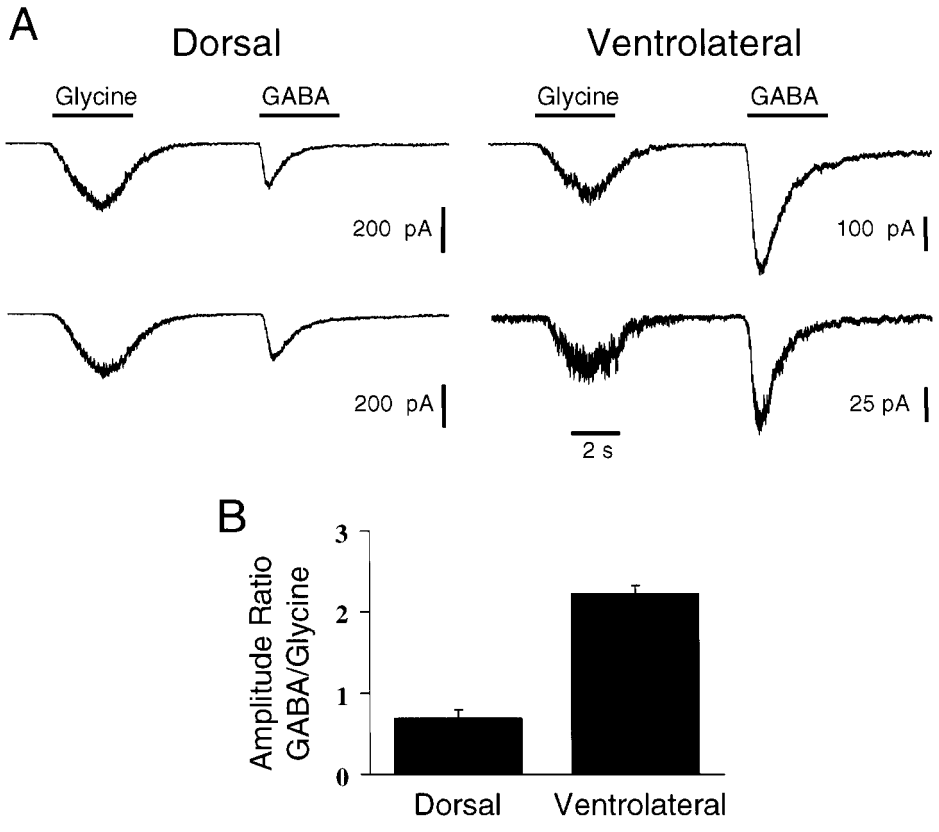

Figure 8. The response to focal application of glycine (200 μM) and GABA (200 μM) onto excised outside-out patches depends on location within the hypoglossal nucleus of juvenile rats. The ratio of GABAergic/glycinergic peak current amplitude is larger in patches from ventrolateral HMs as compared with patches from dorsal HMs. *A*, For patches from the dorsal region ($n = 3$), the peak amplitudes of the GABAergic current were slightly smaller than the amplitude of the glycinergic currents. However, in patches from the ventrolateral region ($n = 3$), the GABAergic current was on average ~2.3 times as large. Data shown are from a P11 rat. These data are summarized in the *bar graph* in *B*. In all three slices studied, the peak amplitude ratio of the GABAergic/glycinergic current was always greater in patches from ventrolateral HMs, when compared with ratios from the dorsal HMs.

Additionally, the amplitude and rise time data from the two regions did not differ significantly (data not shown).

Response amplitude to focal application of glycine and GABA depends on location of HMs

To further test whether the density of glycine and $GABA_A$ receptors present on juvenile HMs could contribute to differences in the responses, we excised outside-out somal patches from HMs located in either the ventrolateral or dorsal region of the hypoglossal nucleus. For comparison, patches in the same slices were excised from neurons in the dorsal motor nucleus of the vagus, because the dorsal motor nucleus of the vagus exhibits high levels of $GABA_A$ receptor α1 staining and low levels of glycine receptor α1 staining (Figs. 1*B*, 2*B*). After excision, we focally applied glycine and GABA in succession to each of the patches for 3 sec via a double-barrel puffer pipette. To minimize variability, the puffer pipette was visualized and kept secure in one location so that multiple patches from a single slice could be aligned similarly with the puffer pipette.

The peak amplitudes of the glycinergic and GABAergic currents were measured for each patch within a given slice. Data were normalized by dividing the peak GABAergic current by the peak glycinergic current for each patch. Data from a single slice are shown in Figure 8. Traces of data from different patches are shown in Figure 8*A*. In patches from the dorsal region, the GABAergic current peak amplitude was on average approximately three-fourths of the glycinergic current peak amplitude, whereas in the ventrolateral region the GABAergic current peak amplitude was more than twice as large as the glycinergic current peak amplitude (Fig. 8*B*). In patches from all three slices studied, the ratio of the GABAergic current peak amplitude to the glycinergic peak amplitude was always significantly greater in the ventrolateral region when compared with the dorsal region ($p < 0.005$). In the dorsal motor nucleus of vagus, where there are high levels of $GABA_A$ receptor staining and very low levels of glycine receptor staining, the GABAergic current peak amplitude was on average almost six times larger than the glycinergic current peak amplitude across all slices studied (data not shown).

Cotransmission of glycine and GABA to HMs in different regions of the hypoglossal nucleus of juvenile rats

After determining that the level of $GABA_A$ receptor α1 subunit labeling was related to the kinetic properties of mIPSCs, we tested whether co-release of glycine and GABA could be measured in both the ventrolateral and dorsal region of the hypoglossal nucleus. Previous work from our laboratory has demonstrated cotransmission to HMs in neonatal (P1–5) animals (O'Brien and Berger, 1999). The current study is focused on the juvenile age group. The results above demonstrated that at this age $GABA_A$ receptor α1 subunit and GABA neurotransmitter labeling appeared to be mismatched. We studied whether this mismatch of receptor and neurotransmitter affected measurements of co-release to HMs. If GABA and glycine were co-released from single vesicles stored in presynaptic terminals and both GABAergic and glycinergic receptors were present at a single synapse, we would predict that mIPSCs should have both a fast decaying glycinergic component and a slow decaying GABAergic component.

To investigate the degree to which cotransmission occurs in different regions of the nucleus, we recorded mIPSCs in the presence of TTX (1 μM), DNQX (20 μM), and AP5 (25 μM). Using pentobarbital (25 μM) to slow the GABAergic mIPSC decay times, we first recorded pure GABAergic and glycinergic mIPSCs in isolation. For the isolated GABAergic and glycinergic events, histogram distributions containing equal numbers (2000)

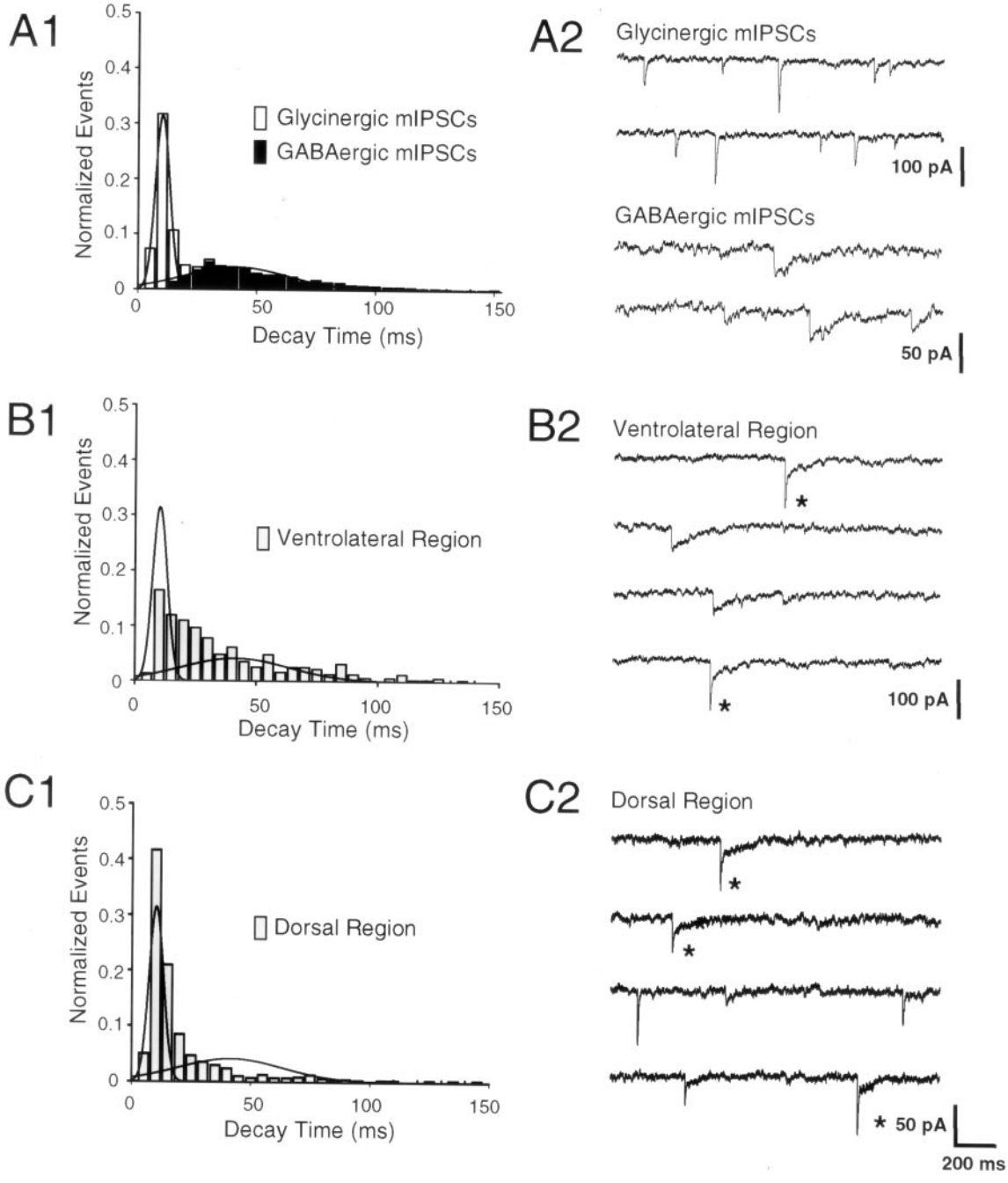

Figure 9. In juvenile HMs, dual component mIPSCs recorded in HMs from the dorsal and ventrolateral regions of the nucleus. *A1*, Normalized histogram distributions of the decay times for pure GABAergic (*black bars*) and pure glycinergic mIPSCs (*white bars*) recorded in isolation in the presence of pentobarbital. For comparison, each distribution, composed of equal numbers of events, is fitted with a Gaussian. *A2*, Raw data of pure GABAergic and glycinergic mIPSCs. *B1*, *C1*, Mixed GABAergic and glycinergic mIPSCs recorded in the presence of pentobarbital in an HM from the ventrolateral region (*B1*) and an HM from the dorsal region (*C1*) of the hypoglossal nucleus. Superimposed on each graph is the Gaussian fit of the pure GABAergic and glycinergic events. *B2*, *C2*, Dual-component mIPSCs having both fast and slow decaying components are present in the raw traces of HMs from both regions (*asterisks*). The calibration shown in *C2* also applies to *A2* and *B2*.

of GABAergic and glycinergic event decay times from different cells were normalized. Data were normalized by dividing each histogram bin by the total number of GABAergic and glycinergic events (4000 events). The GABAergic and glycinergic data were each fitted with a single Gaussian (representing 50% GABAergic mIPSCs and 50% glycinergic mIPSCs) for comparison with mixed mIPSCs recorded in either the dorsal or ventrolateral region (Fig. 9*A1*). Also shown in Figure 9*A2* are single traces showing pure GABAergic and glycinergic mIPSCs. These traces show the short-duration rapidly decaying glycinergic mIPSCs versus the longer-lasting slowly decaying GABAergic mIPSCs.

We then plotted distributions of the decay times of mixed mIPSCs from HMs in either the ventrolateral or dorsal region (Fig. 9, *B1* and *C1*, respectively). The mIPSC decay times distributions from these two juvenile HMs were statistically different (Kolmogorov–Smirnov test; $p < 0.05$). We superimposed the

Gaussian fits of pure GABAergic and glycinergic mIPSCs on each histogram. In the ventrolateral region the frequency distribution of decay times clearly differed from distributions of the pure GABAergic and glycinergic mIPSCs (Fig. 9*B1*). The distribution shown in Figure 9*B1* indicates that there were a large number of events with decay times from ~20 to 30 msec that were not present in the predicted pure GABAergic or pure glycinergic distributions. These results suggest that both $GABA_A$ and glycine receptors contributed to the decay times of many single mIPSCs. In the dorsal region, decay times of mIPSCs had a distribution more similar to the pure GABAergic and pure glycinergic Gaussians (Fig. 9*C1*). However, in both cases when we examined the raw data traces we were able to detect dual component mIPSCs (Fig. 9*B2*,*C2*, *asterisks*). This result suggests that dual-component mIPSCs, caused by co-release of GABA and glycine from single synaptic vesicles, occurred in both ventrolateral and dorsal HMs. However, detection of such events from HMs of the dorsal region via distributions of decay times was more difficult because the GABAergic component in these dual-component events was often very small when compared with the glycinergic component of the mIPSCs.

DISCUSSION

Developmental changes in inhibitory synaptic transmission

Our immunohistochemical studies demonstrate that there are changes in both the $GABA_A$ and glycine receptor subunit staining throughout development. We found that labeling of $GABA_A$ and glycine α1 subunits, normally present in adult HMs (Fritschy and Mohler, 1995; Singer et al., 1998), was weak in the neonatal hypoglossal nucleus. Nevertheless, in a previous study we recorded glycinergic and GABAergic synaptic responses in neonates (O'Brien and Berger, 1999). These data suggest that both $GABA_A$ and glycine receptors are present on neonatal HMs; however, these receptors do not contain the respective α1 subunits. Thus in the neonate, the glycine receptor-mediated responses may arise from glycine receptors expressing α2 subunits that are found (Singer et al., 1998). The $GABA_A$ receptor-mediated events may be caused by $GABA_A$ receptors expressing α2 subunits (Donato and Nistri, 2000).

We recorded $GABA_A$ receptor-meditated mIPSCs throughout the juvenile hypoglossal nucleus and found that the decay times of $GABA_A$ receptor-mediated mIPSCs became faster with postnatal development by comparing the decay times of GABAergic responses from this study with the neonatal decay times from our previous study (O'Brien and Berger, 1999). Other reports have shown that changes in GABAergic mIPSCs decay kinetics reflect changes in receptor desensitization rates (Jones and Westbrook, 1996). In expression systems, changes in desensitization and deactivation are correlated with expression of different subunits (Verdoorn et al., 1990; Gingrich et al., 1995; Tia et al., 1996), suggesting that changes in $GABA_A$ α1 subunit expression in the nucleus with postnatal development could influence response kinetics.

We recorded glycine receptor-mediated mIPSCs and found that the developmental decrease in decay times of GABAergic responses is paralleled by a decrease in the decay times of glycinergic responses (O'Brien and Berger, 1999). Previous work from our laboratory has demonstrated that changes in α subunit expression lead to functional changes in the electrophysiological properties of the glycinergic currents (Singer et al., 1998). In HMs the glycinergic mIPSC decay time shortened with development because of changes in channel deactivation rate. These changes correlated with a decrease in α2 subunit expression and an increase in α1. In HMs the faster kinetics of inhibitory responses with development, as compared with the neonates, may be important for timing of motor output.

Also, throughout the adult (P28–30) nucleus, $GABA_A$ receptor α1 subunit labeling was weaker, whereas glycine receptor α1 subunit labeling was uniform and dense. These data suggest that in adult HMs, glycinergic synaptic transmission is predominant over GABAergic synaptic transmission. It is possible that $GABA_A$ receptors are present on the dendrites of hypoglossal motoneurons that project beyond the hypoglossal nucleus, accounting for measurable GABAergic responses in adult rabbit and cat (Altmann et al., 1972; Takata and Ogata, 1980). However, in other systems inhibited both by GABA and glycine in neonatal neurons, the contribution of GABA decreases during development. In the lateral superior olive of the gerbil auditory system, there is a shift from GABAergic to glycinergic synaptic transmission (Kotak et al., 1998). The decrease in GABAergic synaptic transmission is accompanied by a decrease in the $GABA_A$ receptor β2/3 subunit labeling.

Functional differences between GABAergic and glycinergic synaptic transmission

We compared the kinetics of GABAergic and glycinergic mIPSCs in juvenile HMs and found that the $GABA_A$ receptor-mediated currents decayed significantly slower than glycine responses (even in the absence of pentobarbital). Shunting inhibition arises from an increase in membrane conductance. Overlapping of slower synaptic events, or continuous activation of $GABA_A$ receptors, has been demonstrated in cerebellar granule, hippocampal, and cortical neurons (Staley and Mody, 1992; Brickley et al., 1996; Salin and Prince, 1996). As demonstrated in the hippocampus, shunting inhibition via GABA may be important to preferentially block slower NMDA excitatory currents as compared with faster non-NMDA excitatory currents. (Staley and Mody, 1992). Because the reversal potential for chloride is similar to the resting potential of juvenile HMs (Singer et al., 1998), both $GABA_A$ and glycine receptor activation would result in shunting inhibition, with slower $GABA_A$ receptor-mediated events producing a longer duration shunt.

Differential distribution of $GABA_A$ α1 subunit in the hypoglossal nucleus

In juvenile HMs we found that the $GABA_A$ receptor α1 subunit is differentially distributed within the hypoglossal nucleus. Labeling of the $GABA_A$ receptor α1 subunit was greatest in the ventrolateral region of the nucleus and modest in the dorsal region. This differential distribution of $GABA_A$ receptor α1 subunit labeling is absent in adult HMs. In contrast, the glycine receptor α1 subunit distribution was uniform throughout the nucleus. In juvenile HMs, mIPSCs from the ventrolateral region had slower decay kinetics than mIPSCs from the dorsal region. Outside-out patch current recordings revealed that the ratio of GABAergic to glycinergic currents was larger in the ventrolateral region as compared with the dorsal region. These results suggest that mIPSCs recorded from ventrolateral HMs have larger $GABA_A$ receptor-mediated components.

It is possible that in the dorsal region of the nucleus there were $GABA_A$ receptor subunits expressed that we were unable to detect with the specific antibody used. However, the properties of pure GABAergic mIPSCs recorded from different regions of the

hypoglossal nucleus did not differ. Therefore, we believe that the differences observed in the mixed mIPSCs and outside-out patch responses from different regions of the nucleus were caused by variations in the number of $GABA_A$ receptor-mediated synapses in various regions rather than differences in subunit composition.

What is the functional significance of having different subpopulations of motoneurons with respect to the distribution of $\alpha 1$ subunits of the $GABA_A$ and glycine receptors? The tongue is a complex muscle made up of eight different muscle groups (Lowe, 1980). The hypoglossal nucleus is somatotopically organized. The lateral branch of the hypoglossal nerve contains axons that arise from HMs located in the dorsal portion of the motor nucleus and innervates extrinsic retractor tongue muscles (Dobbins and Feldman, 1995). The medial branch of the hypoglossal nerve has axons from HMs that have cell bodies located in the ventral portion of the hypoglossal nucleus, and the medial branch of the hypoglossal nerve innervates the main protruder tongue muscle (Dobbins and Feldman, 1995; McClung and Goldberg, 1999). Thus motoneurons projecting to the same muscle are located within distinct regions of the hypoglossal nucleus. Muscle compartmentalization of the hypoglossal motor nucleus is found in newborn animals (1–2 d old) and remains present throughout development (Sokoloff, 1993). Differential sensitivity to GABA and glycine of different HMs that innervate different tongue muscles may be important for normal function of these tongue muscles.

Co-release of glycine and GABA onto HMs

We have demonstrated that glycine and GABA are co-released onto both neonatal and juvenile HMs. In specific areas of the juvenile hypoglossal motor nucleus, immunohistochemical studies revealed that glycine receptor $\alpha 1$ subunit labeling remained dense and uniform, whereas $GABA_A$ receptor $\alpha 1$ subunit was weak. These data suggest that in certain regions of the juvenile hypoglossal nucleus, glycine is the predominant inhibitory neurotransmitter. However, GABA neurotransmitter labeling was uniformly present in the juvenile hypoglossal nucleus. In both the dorsal and ventrolateral regions of the juvenile nucleus, where $GABA_A$ receptor labeling was different, dual component mIPSCs were recorded. These data suggest that GABA is co-released with glycine throughout the juvenile hypoglossal nucleus.

What is the function of GABA and glycine co-release? At excitatory synapses, GABA has been shown to act on presynaptic $GABA_B$ receptors, decreasing neurotransmitter release (Bowery et al., 1980). A similar effect of $GABA_B$ receptor activation has also been shown to decrease GABA and glycine receptor-mediated synaptic transmission in several systems (Doze et al., 1995; Khazipov et al., 1995; Kotak et al., 1998; Lim et al., 2000). Anatomical studies have shown that $GABA_B$ receptors are present in the hypoglossal nucleus (Margeta-Mitrovic et al., 1999), and there is physiological evidence that activation of $GABA_B$ receptors can influence responses of HMs. Work by Okabe et al. (1994) suggests that $GABA_B$ receptors located within the hypoglossal nucleus may influence the hypoglossal nerve activity *in vivo*. It is possible that co-release of GABA at glycinergic synapses may activate presynaptic $GABA_B$ receptors in adult and juvenile HMs, located on these or nearby synaptic terminals, thereby reducing $GABA_A$ and glycine receptor-mediated inhibitory neurotransmission.

REFERENCES

Altmann H, Cherubini E, Sonnhof U (1972) Differential strength of action of glycine and GABA in hypoglossus nucleus. Pflügers Arch 331:90–94.

Bowery NG, Hill DR, Hudson AL, Doble A, Middlemiss DN, Shaw J, Turnbull M (1980) (−)Baclofen decreases neurotransmitter release in the mammalian CNS by an action at a novel GABA receptor. Nature 283:92–94.

Brickley SG, Cull-Candy SG, Farrant M (1996) Development of a tonic form of synaptic inhibition in rat cerebellar granule cells resulting from persistent activation of $GABA_A$ receptors. J Physiol (Lond) 497:753–759.

Cochran SL (1993) Algorithms for detection and measurement of spontaneous events. J Neurosci Methods 50:105–121.

Crawford GD, Correa L, Salvaterra PM (1982) Interaction of monoclonal antibodies with mammalian choline acetyltransferase. Proc Natl Acad Sci USA 79:7031–7035.

Dobbins EG, Feldman JL (1995) Differential innervation of protruder and retractor muscles of the tongue in rat. J Comp Neurol 357:376–394.

Donato R, Nistri A (2000) Relative contribution by GABA or glycine to Cl(−)-mediated synaptic transmission on rat hypoglossal motoneurons in vitro. J Neurophysiol 84:2715–2724.

Doze VA, Cohen GA, Madison DV (1995) Calcium channel involvement in GABAB receptor-mediated inhibition of GABA release in area CA1 of the rat hippocampus. J Neurophysiol 74:43–53.

Fritschy JM, Mohler H (1995) $GABA_A$-receptor heterogeneity in the adult rat brain: differential regional and cellular distribution of seven major subunits. J Comp Neurol 359:154–194.

Fritschy JM, Paysan J, Enna A, Mohler H (1994) Switch in the expression of rat $GABA_A$-receptor subtypes during postnatal development: an immunohistochemical study. J Neurosci 14:5302–5324.

Gao BX, Ziskind-Conhaim L (1995) Development of glycine- and GABA-gated currents in rat spinal motoneurons. J Neurophysiol 74:113–121.

Gingrich KJ, Roberts WA, Kass RS (1995) Dependence of the $GABA_A$ receptor gating kinetics on the alpha-subunit isoform: implications for structure-function relations and synaptic transmission. J Physiol (Lond) 489:529–543.

Isaacson JS, Walmsley B (1995) Counting quanta: direct measurements of transmitter release at a central synapse. Neuron 15:875–884.

Jonas P, Bischofberger J, Sandkuhler J (1998) Corelease of two fast neurotransmitters at a central synapse. Science 281:419–424.

Jones MV, Westbrook GL (1996) The impact of receptor desensitization on fast synaptic transmission. Trends Neurosci 19:96–101.

Katz B (1969) The release of neural transmitter substances. Liverpool: Liverpool UP.

Khazipov R, Congar P, Ben Ari Y (1995) Hippocampal CA1 lacunosum-moleculare interneurons: modulation of monosynaptic GABAergic IPSCs by presynaptic $GABA_B$ receptors. J Neurophysiol 74:2126–2137.

Konrat G, Halliday G, Sullivan C, Harper C (1992) Preliminary evidence suggesting delayed development in the hypoglossal and vagal nuclei of SIDS infants: a necropsy study. J Child Neurol 7:44–49.

Kotak VC, Korada S, Schwartz IR, Sanes DH (1998) A developmental shift from GABAergic to glycinergic transmission in the central auditory system. J Neurosci 18:4646–4655.

Lim R, Alvarez FJ, Walmsley B (2000) GABA mediates presynaptic inhibition at glycinergic synapses in a rat auditory brainstem nucleus. J Physiol (Lond) 525:447–459.

Lowe AA (1980) The neural regulation of tongue movements. Prog Neurobiol 15:295–344.

Margeta-Mitrovic M, Mitrovic I, Riley RC, Jan LY, Basbaum AI (1999) Immunohistochemical localization of GABA(B) receptors in the rat central nervous system. J Comp Neurol 405:299–321.

McClung JR, Goldberg SJ (1999) Organization of motoneurons in the dorsal hypoglossal nucleus that innervate the retrusor muscles of the tongue in the rat. Anat Rec 254:222–230.

O'Brien JA, Berger AJ (1999) Cotransmission of GABA and glycine to brainstem motoneurons. J Neurophysiol 82:1638–1641.

Okabe S, Woch G, Kubin L (1994) Role of $GABA_B$ receptors in the control of hypoglossal motoneurons in vivo. NeuroReport 5:2573–2576.

Pfeiffer F, Simler R, Grenningloh G, Betz H (1984) Monoclonal antibodies and peptide mapping reveal structural similarities between the subunits of the glycine receptor of rat spinal cord. Proc Natl Acad Sci USA 81:7224–7227.

Pow DV, Wright LL, Vaney DI (1995) The immunocytochemical detection of amino-acid neurotransmitters in paraformaldehyde-fixed tissues. J Neurosci Methods 56:115–123.

Remmers JE, Anch AM, deGroot WJ, Baker Jr JP, Sauerland EK (1980) Oropharyngeal muscle tone in obstructive sleep apnea before and after strychnine. Sleep 3:447–453.

Salin PA, Prince DA (1996) Spontaneous $GABA_A$ receptor-mediated inhibitory currents in adult rat somatosensory cortex. J Neurophysiol 75:1573–1588.

Simon M, Horcholle-Bossavit G (1999) Glycine- and GABA-immunoreactive nerve terminals apposed to alpha-motoneurons during postnatal development in kittens: a quantitative study using the detector. Exp Brain Res 129:229–240.

Singer JH, Berger AJ (1999) Contribution of single-channel properties to the time course and amplitude variance of quantal glycine currents recorded in rat motoneurons. J Neurophysiol 81:1608–1616.

Singer JH, Talley EM, Bayliss DA, Berger AJ (1998) Development of glycinergic synaptic transmission to rat brainstem motoneurons. J Neurophysiol 80:2608–2620.

Sokoloff AJ (1993) Topographic segregation of genioglossus motoneurons in the neonatal rat. Neurosci Lett 155:102–106.

Staley KJ, Mody I (1992) Shunting of excitatory input to dentate gyrus granule cells by a depolarizing $GABA_A$ receptor-mediated postsynaptic conductance. J Neurophysiol 68:197–212.

Sumi T (1969) Functional differentiation of hypoglossal neurons in cats. Jpn J Physiol 19:55–67.

Sumino R, Nakamura Y (1974) Synaptic potentials of hypoglossal motoneurons and a common inhibitory interneuron in the trigemino--hypoglossal reflex. Brain Res 73:439–454.

Takata M, Ogata K (1980) Two components of inhibitory postsynaptic potentials evoked in hypoglossal motoneurons by lingual nerve stimulation. Exp Neurol 69:299–310.

Tia S, Wang JF, Kotchabhakdi N, Vicini S (1996) Distinct deactivation and desensitization kinetics of recombinant GABAA receptors. Neuropharmacology 35:1375–1382.

Umemiya M, Berger AJ (1994) Properties and function of low- and high-voltage-activated Ca^{2+} channels in hypoglossal motoneurons. J Neurosci 14:5652–5660.

Verdoorn TA, Draguhn A, Ymer S, Seeburg PH, Sakmann B (1990) Functional properties of recombinant rat GABAA receptors depend upon subunit composition. Neuron 4:919–928.

Vitorica J, Park D, de Blas AL (1990) The GABAA/benzodiazepine receptor complex in rat brain neuronal cultures. Characterization by immunoprecipitation. Brain Res 537:209–215.

Yamuy J, Fung SJ, Xi M, Morales FR, Chase MH (1999) Hypoglossal motoneurons are postsynaptically inhibited during carbachol-induced rapid eye movement sleep. Neuroscience 94:11–15.